The cholinergic antagonist α-bungarotoxin also binds and blocks a subset of GABA receptors

Corey M. McCann*, John Bracamontes†, Joe Henry Steinbach†, and Joshua R. Sanes*‡

*Department of Molecular and Cellular Biology, Harvard University, Cambridge, MA 02138; and †Department of Anesthesiology, Washington University School of Medicine, St. Louis, MO 63110

Contributed by Joshua R. Sanes, February 2, 2006

The polypeptide snake toxin α-bungarotoxin (BTX) has been used in hundreds of studies on the structure, function, and development of the neuromuscular junction because it binds tightly and specifically to the nicotinic acetylcholine receptors (nAChRs) at this synapse. We show here that BTX also binds to and blocks a subset of $GABA_A$ receptors ($GABA_A$Rs) that contain the $GABA_A$R β3 subunit. These results introduce a previously unrecognized tool for analysis of $GABA_A$Rs but may complicate interpretation of some studies on neuronal nAChRs.

acetylcholine | neurotransmitter | synapse

Perhaps the best understood of all synapses is the vertebrate skeletal neuromuscular junction (1). Although the accessibility, simplicity, and large size of this synapse are often viewed as its principle advantages, another important factor has been the availability of a highly versatile ligand for the nicotinic acetylcholine receptors (nAChRs) that are the critical component of its postsynaptic membrane. This ligand, α-bungarotoxin (BTX), is a 74-aa polypeptide derived from the venom of the banded krait, *Bungarus multicinctus.* BTX binds quasi-irreversibly and highly specifically to the nAChRs at the neuromuscular junction and in electric organs of *Torpedoes* and rays (2, 3). An additional advantage is that it is readily derivatized without loss of activity; it has been conjugated to agarose for affinity-purification of AChRs (4), to ^{125}I for quantification of AChRs (5), and to fluorophores for tracking of AChRs during synaptogenesis (ref. 6; see refs. 3 and 7 for reviews of early and recent work, respectively).

BTX binds not only to the α1 subunit contained in muscle nAChRs but also to a subset of neuronal nAChRs; it binds those containing the α7–α10 subunits but not those containing the α2–α6 subunits (8, 9). As at the neuromuscular junction, studies of the structure, function, and development of neuronal cholinergic synapses have benefited from BTX.

In studies on both muscle and neuronal cholinergic synapses, a guiding assumption has been that BTX binds only to nAChRs. During the course of studies to label neurotransmitter receptors that had been tagged with a BTX-binding motif (10), we obtained evidence that challenged this premise. We show here that BTX binds to a subset of $GABA_A$ receptors ($GABA_A$Rs). In particular, BTX blocks $GABA_A$Rs that contain interfaces between adjacent β3 subunits.

Results

BTX Binds to a $GABA_A$R Subunit in Heterologous Cells. In initial studies, we found that fluorophore-conjugated BTX stained human embryonic kidney (HEK 293) cells that had been transfected with a cDNA encoding the rat $GABA_A$R β3 subunit (Fig. 1*a*). This staining was not seen in untransfected cells (Fig. 1*a*). Staining by fluorophore-conjugated BTX was blocked by preincubation with unconjugated BTX, whereas staining was seen when cells were incubated successively with BTX, an affinity-purified antibody to BTX, and fluorophore-conjugated second antibody (Fig. 1*a* and data not shown). Similar results were obtained in several cell types, and specific staining was observed when cells were stained live or after fixation and permeabilization (Fig. 1 *b* and *c*). Staining by BTX and by an antibody to $GABA_A$R β3 overlapped (Fig. 1*d*). These results show that BTX binds to $GABA_A$R β3.

To assess the affinity of BTX for $GABA_A$R β3, we used quantitative fluorescence microscopy, as described in ref. 10, to measure BTX binding to stably transfected HEK 293 cells. The apparent K_d determined in this way was $\approx$50 nM (Fig. 2*a*). We also used this assay to pharmacologically characterize BTX binding to $GABA_A$R β3. Binding was affected little by ligands for nAChRs containing the α1 (hexamethonium or nicotine) or α7 (methyllycaconitine) subunits or by the $GABA_A$R modulator pentobarbital (Fig. 2*b*). In contrast, binding of BTX to $GABA_A$R β3-expressing cells was significantly reduced in the presence of the $GABA_A$R antagonist bicuculline (Fig. 2*b*).

BTX Binds Selectively to the $GABA_A$R β3 Subunit. To determine whether other $GABA_A$R subunits also bound BTX, we expressed rat $GABA_A$R β1, β2, β3, α2, or γ2 subunits in HEK cells and then stained cells live or after fixation and permeabilization. Only cells that expressed $GABA_A$R β3 detectably bound BTX (Fig. 3*a*). Because pharmacological and physiological differences between rodent and human $GABA_A$R β-subunits have been reported (11–13), we also tested cells expressing human subunits. Human $GABA_A$R β3 bound BTX, but human $GABA_A$R β1 did not (Fig. 3*b*). Because some subunits ineffectively form channels when expressed on their own (13, 14), we also tested mutant $GABA_A$R β1 subunits with an enhanced ability to form homooligomers and reach the cell surface (J.B. and J.H.S, unpublished data). These $GABA_A$R β1 mutants reached the surface efficiently (as shown by staining for an extracellular epitope tag; see Fig. 3*c Right*) but failed to bind BTX (Fig. 3*c Left*), ruling out the possibility that differential binding of β1 and β3 subunits was secondary to an inability to multimerize.

BTX Binds to the Amino-Terminal Extracellular Domain of $GABA_A$R β3. We exploited the difference between $GABA_A$R β1 and β3 subunits to localize the BTX-binding site. BTX bound to chimeric $GABA_A$R subunits (11) in which the amino-terminal extracellular domain of $GABA_A$R β1 was replaced by the corresponding domain of $GABA_A$R β3, whereas no binding was detected to chimeras in which the amino-terminal extracellular domain of $GABA_A$R β3 was replaced by the corresponding domain of $GABA_A$R β1 (Fig. 3*d*). From these results, we conclude that BTX binds to the amino-terminal extracellular domain of $GABA_A$R β3. Knowing that BTX also binds to an amino-terminal site in nAChR α1 and α7 subunits (15–17),

Conflict of interest statement: No conflicts declared.

Abbreviations: BTX, α-bungarotoxin; $GABA_A$R, $GABA_A$ receptor; nAChR, nicotinic acetylcholine receptor; MEQ, 6-methoxy-*N*-ethylquinolium iodide.

‡To whom correspondence should be addressed at: Department of Molecular and Cellular Biology, Harvard University, 7 Divinity Avenue, Cambridge, MA 02138. E-mail: sanesj@mcb.harvard.edu.

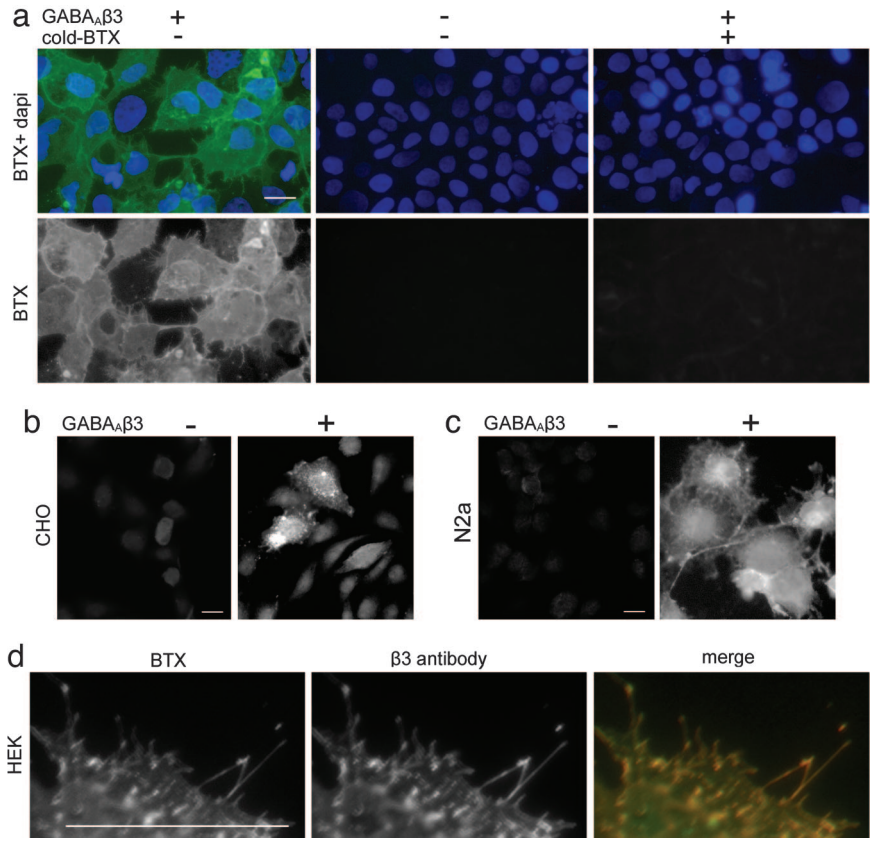

Fig. 1. BTX binds to GABA$_A$β3. (*a*) Rhodamine-BTX labels HEK 293 cells transfected with a plasmid encoding GABA$_A$R β3. Labeling is blocked by preincubation with unconjugated BTX. Untransfected cells are not labeled. (*b* and *c*) BTX specifically labels GABA$_A$R β3-transfected CHO and N2a cells. (*d*) Labeling of GABA$_A$R β3-transfected cells by BTX and anti-GABA$_A$R β3 antibody is coincident. Cells in *a* and *d* were stained live and then fixed; cells in *b* and *c* were fixed and permeabilized before staining. (Scale bars, 5 μm.)

which are distantly related to GABA$_A$Rs, we compared nAChR and GABA$_A$R sequences. Surprisingly, GABA$_A$R β3 did not share residues critical for BTX binding to nAChRs, and no distinctive differences between GABA$_A$R β1 and β3 sequences occurred in this domain (Fig. 8, which is published as supporting information on the PNAS web site). BTX may therefore bind to a previously uncharacterized motif on GABA$_A$R β3. As discussed below, the binding site may involve an interface between adjacent β3 subunits.

BTX Blocks Chloride Conductance Through GABA$_A$R β3 Receptors. Knowing that BTX blocks activation of nAChRs, we asked whether BTX binding also affected the function of GABA$_A$Rs. Because GABA$_A$Rs are selectively permeable to chloride ions, we used the chloride indicator 6-methoxy-*N*-ethylquinolium iodide (MEQ), the fluorescence of which decreases as chloride concentration increases (18). When chloride levels in the medium bathing control HEK 293 cells were increased, a minimal change in MEQ fluorescence was observed (Fig. 4). In contrast, MEQ fluorescence decreased significantly when chloride was added to the medium bathing HEK 293 cells that had been stably transfected with GABA$_A$R β3 (80 ± 10% decrease; Fig. 4). When chloride was added to the medium in the presence of BTX, MEQ fluorescence changed little (10 ± 5% decrease; Fig. 4). BTX had no effect on MEQ fluorescence in untransfected

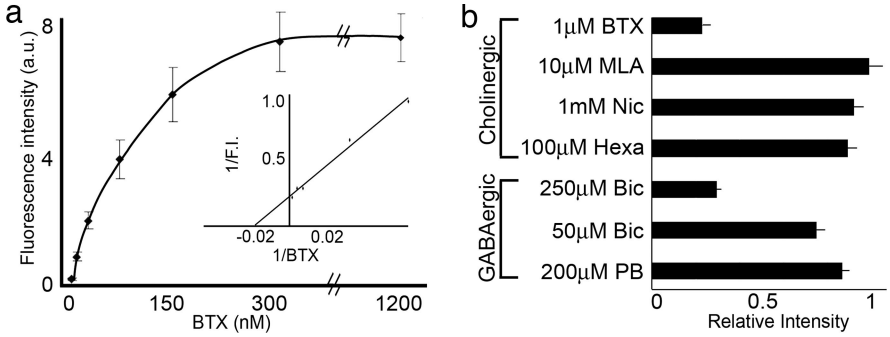

Fig. 2. Quantitative assessment of BTX binding to GABA$_A$R β3-expressing HEK 293 cells. (*a*) BTX binding to a stably transfected cell line was measured by quantitative fluorescence microscopy (10). (*Inset*) Double-reciprocal plot shows that $K_d \approx 50$ nM. (*b*) BTX binding to this cell line was insensitive to preincubation with blockers of nAChRs containing α1 or α7 subunits [methyllycaconitine (MLA), nicotine (Nic), and hexamethonium (Hexa)] or the GABA$_A$R modulator pentobarbital (PB) but was blocked by the GABA$_A$R antagonist bicuculline (Bic).

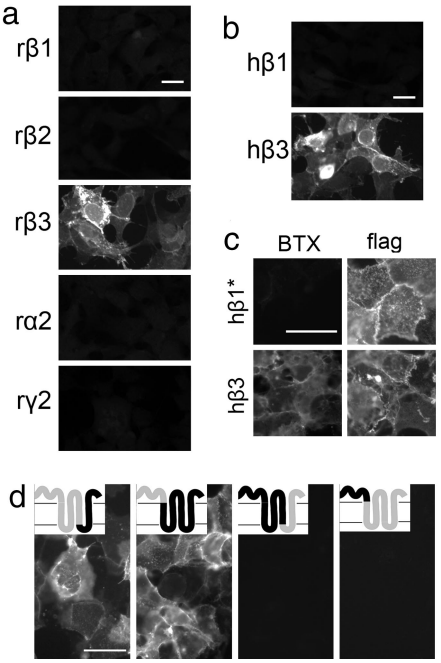

Fig. 3. Mapping of BTX-binding sites on $GABA_AR$s. HEK 293 cells transfected with cDNAs encoding indicated subunits were stained with BTX after (*a*, *b*, and *d*) or before (*c*) fixation and permeabilization. (*a*) Rat (r) $GABA_AR$ $\beta3$ binds BTX, but rat $GABA_AR$ $\beta1$, $\beta2$, $\alpha2$, and $\gamma2$ do not. (*b*) Human (h) $GABA_AR$ $\beta3$ binds BTX, but human $GABA_AR$ $\beta1$ does not. (*c*) A $GABA_AR$ $\beta1$ subunit that had been mutated to enhance its ability to form pentamers ($\beta1$*) failed to bind BTX. The subunit bore an amino-terminal ''flag'' epitope tag; antibody to the tag stained live cells, confirming that the subunit reached the cell surface. A similarly tagged wild-type $\beta3$ subunit did bind BTX. (*d*) Chimeric receptors containing the amino-terminal extracellular domain of $GABA_AR$ $\beta3$ fused to the remainder of $GABA_AR$ $\beta1$ bind BTX, but chimeras containing the amino-terminal extracellular domain of $GABA_AR$ $\beta1$ fused to the remainder of $GABA_AR$ $\beta3$ do not. (*Insets*) Portions of receptors derived from $\beta3$ (gray) and $\beta1$ (black); fusions are at amino acid 314 in the first and third chimeras and at amino acid 213 in the second and fourth chimera (11). (Scale bars, 5 μm.)

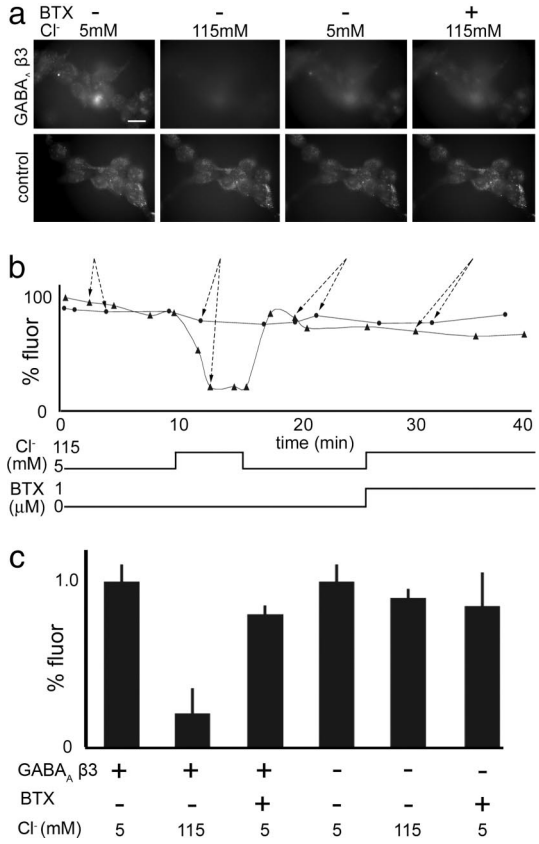

Fig. 4. BTX blocks chloride influx in a $GABA_AR$ $\beta3$-expressing HEK 293 cell line. (*a*) Micrographs of cells incubated with the chloride sensor MEQ. (*Upper*) In cells stably transfected with $GABA_AR$ $\beta3$, MEQ fluorescence decreases when the extracellular chloride concentration is increased. The decrease is blocked by BTX. (*Lower*) Untransfected control HEK 293 cells show minimal response to changes in extracellular chloride concentration. (Scale bar, 5 μm.) (*b*) Quantitation of fluorescent signals from the experiment in *a*. ●, control; ▲, $GABA_AR$. Arrows show correspondence between micrographs in *a* and points in *b*. (*c*) Average MEQ fluorescence intensity in media containing 5 mM or 115 mM Cl^- in the presence or absence of 1 μM BTX. Measurements in 115 mM Cl^- were made 5 min after switching from 5 mM. Bars show mean ± SEM of measurements from 10–20 cells from five experiments.

control cells. These results suggest that $GABA_AR$ $\beta3$ mediates a chloride conductance that can be blocked by BTX. The observation that homooligomeric $\beta3$-$GABA_A$Rs are permeable to chloride in the absence of GABA is consistent with results of some (12) but not all (11) previous electrophysiological studies.

During the course of these experiments, we noted that cells expressing $GABA_AR$ $\beta3$ were more elongated than untransfected cells (Fig. 5*a*). We hypothesized that this difference resulted from the $GABA_AR$-dependent chloride permeability documented above. To test this idea, we cultured cells in the presence or absence of BTX for 48 h and then measured cell shape. Chronic treatment with BTX decreased process length in $GABA_AR$ $\beta3$-expressing cells but had no effect on the shape of untransfected cells (Fig. 5).

Analysis of Homooligomeric GABA $\beta3$ Receptors in *Xenopus* Oocytes. For a more detailed analysis of the effect of BTX on $GABA_AR$ function, we performed voltage clamp analysis of *Xenopus* oocytes that had been injected with $GABA_AR$ $\beta3$ mRNA. $\beta3$ subunits formed channels that were open in the absence of GABA: the conductance of $\beta3$-injected oocytes was ≈40-fold higher than that of controls (118 ± 68 μS, $n = 16$ vs. 3.0 ± 1.5 μS, $n = 4$; $P < 0.00001$ by t test). This conductance was blocked >90% by the $GABA_AR$ antagonist picrotoxin (reduced to 5.3 ± 3.2 μS, $n = 16$) and enhanced more than 5-fold by the $GABA_AR$ modulator pentobarbital (Fig. 6 *a* and *b*). Paradoxically, the picrotoxin-sensitive conductance was inhibited ≈70% by GABA; we cannot explain the discrepancy between this result and previous results (11–13), which showed $GABA_AR$ $\beta3$ homomeric channels to be either activated by or insensitive to GABA. Application of BTX had no detectable effect on the conductance of control eggs ($P = 0.34$) but decreased the picrotoxin-sensitive conductance of $\beta3$-injected eggs by >80% (Fig. 6 *a* and *b*). The effect appeared rapidly (forward rate constant = 23,000 $M^{-1}{\cdot}s^{-1}$) and was slowly reversed after wash-off ($t_{1/2}$ ≈ 10 min; Fig. 6*d*). The K_d calculated from these data, ≈100 nM, was similar to that determined directly (≈50 nM; Fig. 2*a*). BTX also decreased activation by pentobarbital (≈46% decrease, $n = 10$; Fig. 6*a*).

We also tested the effect of BTX on $GABA_AR$ $\beta1$ homooligomers expressed in oocytes. $\beta1$ subunits formed channels that were blocked by picrotoxin (585 ± 470 μS vs. 30 ± 27 μS) and GABA (Fig. 6*c*). However, consistent with binding data reported above (Fig. 3), these channels were minimally sensitive to BTX (Fig. 6 *c* and *d*).

BTX Blocks $GABA_AR$ $\beta3$ Channels Containing a $\beta3/\beta3$ Interface. Although homooligomeric $GABA_A$Rs are functional in nonneuronal cells, most $GABA_A$Rs in neurons are composed of α-, β-, and γ-subunits (13). To ask whether BTX blocks heterooligo-

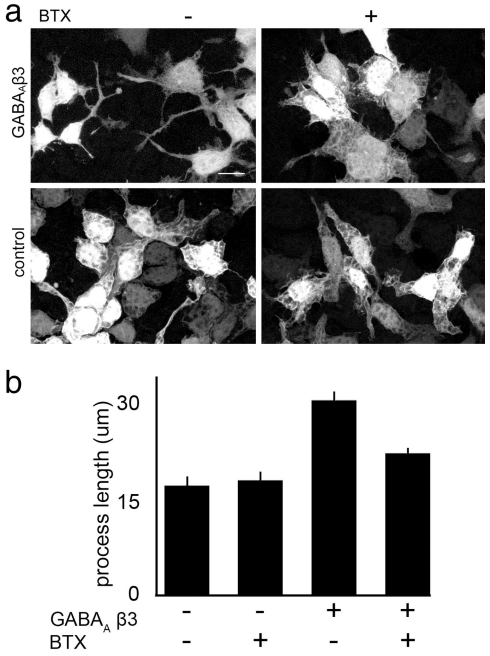

Fig. 5. BTX prevents the elongation of HEK 293 cells stably transfected with $GABA_AR$ $\beta3$. (*a*) Cellular processes in HEK 293 cells stably transfected with $GABA_AR$ $\beta3$ are longer than those in untransfected cells. Prolonged incubation with BTX shortens processes in cells stably transfected with $GABA_AR$ $\beta3$ but not in untransfected cells. All cells were transiently transfected with a plasmid encoding EGFP to label a subset of the cells in a field. (Scale bar, 5 μm.) (*b*) Quantification of process length. Measurements were made from the nucleus to the distalmost portion of a process. Bars show mean ± SEM of measurements from 150–200 cells from two experiments.

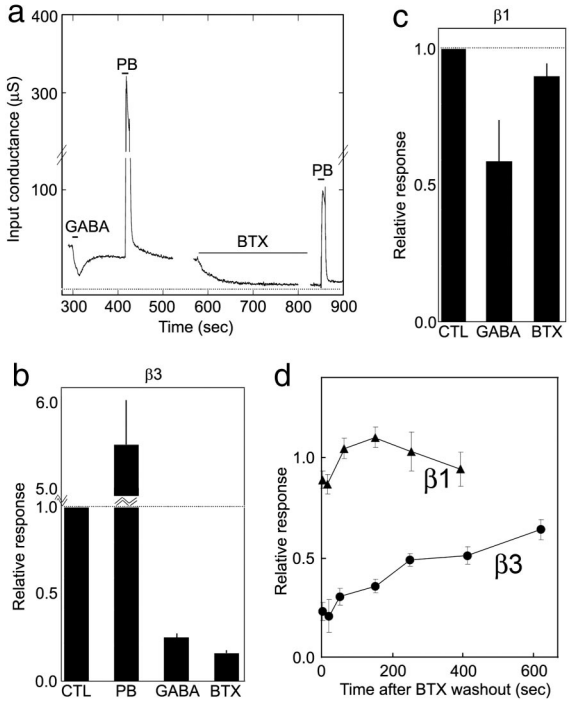

Fig. 6. Effect of BTX on $GABA_AR$ currents recorded from *Xenopus* oocytes injected with mRNAs encoding $GABA_AR$ subunits. (*a*) Channels formed by $GABA_AR$ $\beta3$ are spontaneously open (12); conductance is blocked by 100 μM GABA or 1 μM BTX and potentiated by 100 μM pentobarbital (PB). Dotted line shows conductance after addition of 100 μM picrotoxin. (*b*) Quantification of effects of PB, GABA, and BTX on oocytes expressing $GABA_AR$ $\beta3$, obtained as in *a*; data are averaged from 13 oocytes. (*c*) Similar pharmacological analysis of channels formed by $GABA_AR$ $\beta1$ subunits; data are averaged from eight oocytes. (*d*) Recovery of picrotoxin-sensitive conductance in $GABA_AR$ $\beta1$- and $\beta3$-expressing oocytes after removal of BTX. Data are normalized to the preceding holding conductance.

meric $GABA_ARs$, we analyzed oocytes that had been coinjected with $GABA_AR$ $\alpha1$, $\beta3$, and $\gamma2$ RNAs. As expected (11, 13), GABA activated the resulting receptors, but BTX had no significant effect either on the ligand-independent conductance of the oocytes or on the response to GABA (Fig. 7).

Based on previous studies, the probable composition of these heterooligomeric receptors is $[\alpha1]_2[\beta3]_2[\gamma2]_1$ in the order $\alpha1$-$\beta3$-$\gamma2$-$\alpha1$-$\beta3$ (19–22). They are therefore unlikely to contain adjacent $\beta3$ subunits. The lack of effect of BTX on these receptors could indicate either that BTX is unable to antagonize the effects of GABA or that BTX binds to an interface between adjacent $\beta3$ subunits. To distinguish these possibilities, we analyzed oocytes injected with only $GABA_AR$ $\alpha1$ and $\beta3$ RNAs. The oocytes exhibited GABA-activated currents, presumably mediated by $GABA_ARs$ containing both $\alpha1$ and $\beta3$ subunits. The composition of these receptors is likely to be $[\alpha1]_2[\beta3]_3$ (19, 22), so they would be expected to bear a $\beta3/\beta3$ interface. BTX significantly blocked activation of these receptors by GABA (Fig. 7), supporting the idea that BTX binds to an interface between adjacent $\beta3$ subunits.

Discussion

We have shown that BTX binds not only to a subset of nAChRs but also to a subset of $GABA_ARs$, specifically, those containing an interface between two $GABA_AR$ $\beta3$ subunits. These results are significant in three respects.

First, although genetic and pharmacological studies clearly show that most BTX-binding sites in brain correspond to $\alpha7$ nAChRs (23, 24), our results raise the possibility that some are $GABA_ARs$. This possibility is of particular interest, given the colocalization of nAChRs and $GABA_ARs$ at a subset of GABAergic synapses (25, 26). Moreover, a brief report[§] demonstrates that embryonic muscle cells express $GABA_ARs$. Although the subunit composition of these receptors has not yet been reported, it may be necessary to consider whether some of the BTX binding to newly formed myotubes is to $GABA_ARs$.

Second, because the amino-terminal extracellular domain of $GABA_AR$ $\beta3$ does not contain significant homology to sequences on AChRs known to bind BTX (Fig. 8), $GABA_AR$ $\beta3$ may contain a previously uncharacterized BTX-binding sequence. This sequence could add to existing knowledge on the structures underlying BTX-binding peptides (27) and help to elucidate structural similarities between AChRs and $GABA_ARs$.

Third, BTX appears to bind to $GABA_ARs$ with adjacent $\beta3$ subunits but not to heterooligomeric receptors composed of α-, β-, and γ-subunits. Most $GABA_ARs$ reported in neurons to date are believed to include α-, β-, and γ- or α-, β-, and δ-subunits (13). However, we are aware of no studies that have directly tested the possibility that α/β-containing $GABA_ARs$ or homomeric β-containing $GABA_ARs$ are present in the brain (13). It is important to note that homomeric $\beta3$-$GABA_ARs$ inactivated by GABA would almost certainly have escaped detection in cells that also bear heterooligomeric receptors, which are activated by GABA. BTX may be a useful reagent with which to seek such receptors in neurons.

[§]Borodinsky, L. N. & Spitzer, N. C. (2005) *2005 Abstract Viewer and Itinerary Planner* (Society for Neuroscience, Washington, DC), Program 27.1 (abstr.).

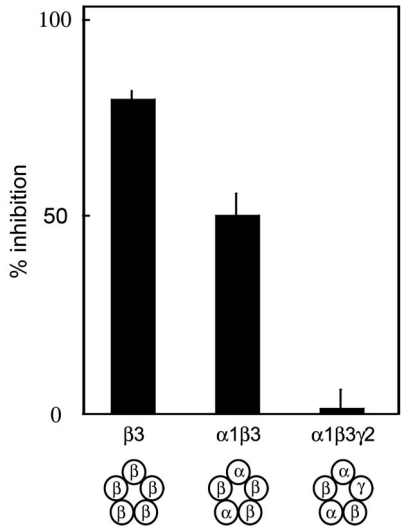

Fig. 7. BTX blocks conductance through $GABA_AR$s with a $\beta3/\beta3$ interface. RNAs encoding indicated combinations of $GABA_AR$ $\alpha1$, $\beta3$, and $\gamma2$ subunits were injected into *Xenopus* oocytes, and current passage was measured before and after application of BTX. Schematics at bottom show predicted pentameric structures for each combination of $GABA_AR$ subunits. Note that a functional block was observed only for $GABA_AR$s predicted to contain an interface between two $\beta3$ subunits. Data are normalized to the response before BTX application. Bars show mean ± SEM from $n = 4–13$ oocytes.

Methods

Transfection and Staining of Cell Lines. Eight-well chamber slides (Lab-Tek) were coated with rat-tail collagen in 30% ethanol. HEK 293, CHO, and N2a cells (American Type Culture Collection) were plated at 2×10^4 cells per well and cultured in DMEM containing 10% FCS. Glutamine (1 mM) was added to medium for N2a and CHO cells. After growth overnight, cells were transfected by using Lipofectamine 2000 (Invitrogen) according to the manufacturer's protocol. Plasmids encoding $GABA_AR$ subunits were obtained from the following sources: rat $\alpha1$ and $\beta2$ were from A. Tobin (University of California, Los Angeles); human $\beta1$ and rat $\gamma2L$ were from D. Weiss (University of Alabama at Birmingham); rat $\beta3$, $\alpha2$, and $\gamma2$ were from P. Seeburg (Max Planck Institute for Medical Research, Heidelberg); human $\beta3$ was from G. White (Neurogen, Branford, CT); and rat $\beta1$ and $\beta1/\beta3$ chimeras were from L. Zhang (National Institutes of Health, Bethesda).

Cells were stained 36–48 h after transfection. Cells were stained in one of several ways: (*i*) For live staining, rhodamine-α-BTX (Molecular Probes) or anti-$GABA_AR$ $\beta3$ (MAB341, Chemicon) was added to media (2 μg/ml and 10 μg/ml final concentration, respectively) for 30 min at 37°C. Cells were then washed two times with media and fixed with 2% paraformaldehyde, rinsed with PBS containing a nuclear dye (DAPI), and mounted in 10% glycerol containing *p*-phenylenediamine. Where appropriate, a second antibody was added after fixation and before mounting. (*ii*) Alternatively, cells were fixed, washed, and incubated for 1 h in 0.1% Triton X-100/2% normal goat serum/2% BSA in PBS and then incubated in rhodamine-α-BTX (as above). (*iii*) In some cases, cells were incubated live with BTX and then fixed and incubated successively with rabbit antibodies to affinity-purified BTX (28) and Cy3-conjugated secondary antibody (Jackson ImmunoResearch). Images were taken on a Zeiss Axiovert epifluorescence microscope.

Quantitative Assessment of BTX Binding. The apparent affinity of BTX for $GABA_AR$s was assessed as described in ref. 10. HEK cells were transfected with a $GABA_AR$ $\beta3$ plasmid that incorporated a neomycin resistance gene. Stably transfected cells were selected with G418, single cells were cloned, and clones expressing the construct in most or all cells were identified. Cells were plated in eight-well chamber slides, stained live at room temperature for 30 min with rhodamine-BTX, and then washed and fixed as above. Images were taken by using a ×10, 0.3 numerical aperture objective. Exposure times and illumination settings were selected to avoid saturated pixels in the wells stained with the highest concentration of probe. Using the same settings, multiple images were taken for each concentration of probe. Using METAMORPH software (Universal Imaging, Downingtown, PA), background values taken from images of identically stained untransfected cells were subtracted from images of transfected cells. Intensity histograms of the entire field were taken, and the most frequent pixel intensity of the histogram was recorded. K_d values were calculated from double reciprocal plots.

To assess pharmacological blockade of BTX binding, the $GABA_AR$ $\beta3$-expressing HEK 293 cell line was preincubated with blocker in DMEM for 20 min and then incubated in the same concentration of blocker along with 1 μg/ml rhodamine-BTX. Fluorescence intensity was then assessed as above.

Sequence Alignment. Sequences of rat AChR $\alpha1$, AChR $\alpha7$, $GABA_AR$ $\beta1$, $\beta2$, and $\beta3$, and *Torpedo* AChR $\alpha1$ were obtained from GenBank. Amino-terminal extracellular domains were identified by Swiss-Prot, and their sequences were aligned by using the AlignX algorithm of VECTORNTI 9.0 (Invitrogen).

Imaging Chloride Concentrations in HEK Cells. Stably transfected and control HEK 293 cells were plated on plastic tissue culture dishes (Nunc) coated with collagen, as described above. diH-MEQ (Molecular Probes) was prepared and applied to HEK 293 cells according to the manufacturer's protocol. Chloride concentration was manipulated by changing the extracellular solution with a syringe pump (Harvard Apparatus) and aspirator. The high- and low-chloride solution contained 110 mM NaCl or $NaNO_3$, respectively, plus 5 mM KCl in 25 mM Hepes buffer (pH 7.2–7.4). Quantitative fluorescence was performed as above by using a water immersion objective (×40, 0.8 numerical aperture).

Morphological Change by BTX Incubation of Stably Transfected Cells. HEK cells stably expressing $GABA_AR$ $\beta3$ were transiently transfected with a plasmid encoding EGFP (Clontech) to facilitate evaluation of cell shape. After transfection, cells were incubated in 4 μg/ml unlabeled BTX (Molecular Probes) for 48 h and then washed, fixed, and imaged. Process length of transfected cells was quantified by using Zeiss LSM 510 software.

Expression in *Xenopus* Oocytes and Physiology. Receptors were expressed in *Xenopus* oocytes by injecting cRNA produced by using the mMessage mMachine T7 Ultra kit (Ambion, Austin, TX). Oocytes were injected with 19 nl of solution containing $GABA_AR$ $\beta1$ or $GABA_AR$ $\beta3$ cRNA at ≈1 μg/ml and incubated at 17°C in ND-96 solution. The $GABA_AR$ $\beta3$ subunit forms functional homomeric receptors with high efficiency. Therefore, when mixtures of subunits were injected, weight ratios of 2:1 and 2:1:4 were used for $\alpha1$:$\beta3$ and $\alpha1$:$\beta3$:$\gamma2L$, respectively, to enhance formation of heteromeric receptors.

Responses were recorded 1–3 days after injecting the oocytes by using a two-electrode oocyte clamp (Warner Instruments, Hamden, CT). Electrodes were filled with 3 M KCl and had resistances of 0.5–1 MΩ. The bath solution contained 96 mM NaCl, 2 mM KCl, 1 mM $MgCl_2$, 1.8 mM $CaCl_2$, and 10 mM Hepes; pH was adjusted to 7.5 with NaOH. The bath had a volume of ≈0.1 ml and was perfused with saline or drug solutions at ≈7 ml/min.

Responses and steady-state activity were measured by estimating the oocyte input conductance by using 400-ms, 10-mV

hyperpolarizing pulses. Pulses were applied by using PCLAMP software (Axon Instruments, Union City, CA), and currents were filtered at 20 Hz and acquired by using a Digidata-1200B (Axon Instruments) at 20 samples per s. Subsequently, the current during the last 150 ms of each pulse was averaged, and then values were interpolated and subtracted to provide an estimate of input conductance by using PCLAMP and EXCEL (Microsoft). Analysis was performed by using EXCEL and SIGMAPLOT (SSPS, Chicago).

Membrane conductance was measured continuously during the exposure to BTX. The effect of BTX was quantified by calculating the amount of picrotoxin-sensitive holding current present at the end of an ≈4-min application of 1 μM BTX relative to that immediately before the application (ratio). The apparent association rate was estimated from a semilogarithmic plot of the first 30 s of BTX exposure (β1: 0.002 ± 0.0004 s^{-1}, $n = 8$; β3: 0.023 ± 0.0027 s^{-1}, $n = 13$).

The recovery of baseline conductance after BTX treatment was relatively slow for β3 receptors. Because of the presence of a consistent diminution of both baseline conductance and pentobarbital responses ("rundown") over time, recovery could not be quantified directly. However, the decline in picrotoxin-sensitive conductance could be described by a single exponential. Accordingly, the recovery was assessed by comparing the observed baseline current to the predicted current.

Oocytes expressing heteromeric receptors had significantly lower input conductance than homomeric β3 receptors (α1β3: 2.0 ± 0.2 μS, $n = 7$; $\alpha\beta3\gamma$2L: 15 ± 4 μS, $n = 6$; for both, $P < 0.00002$ for difference to β3 homomers) and a lower fraction of picrotoxin-sensitive conductance (28% and 57%, respectively). Responses were tested by using 10 μM GABA to avoid any contributions from possible homomeric β3 receptors.

We thank P. Seeburg, A. Tobin, D. Weiss, and G. White for providing $GABA_AR$ cDNAs; L. Zhang for the $GABA_AR$ $\beta1/\beta3$ chimeras; and J. Brubaker for preparation of diH-MEQ. This work was supported by grants from the National Institutes of Health (to J.R.S. and J.H.S.). J.H.S. is the Russell and Mary Shelden Professor of Anesthesiology.

1. Sanes, J. R. & Lichtman, J. W. (1999) *Annu. Rev. Neurosci.* **22,** 389–442.
2. Lee, C. Y., Tseng, L. F. & Chin, T. H. (1967) *Nature* **215,** 1177–1178.
3. Fambrough, D. M. (1979) *Physiol. Rev.* **59,** 165–227.
4. Changeux, J. P., Meunier, J. C. & Huchet, M. (1971) *Mol. Pharmacol.* **7,** 538–553.
5. Fertuck, H. C. & Salpeter, M. M. (1976) *J. Cell Biol.* **69,** 144–158.
6. Anderson, M. J. & Cohen, M. W. (1977) *J. Physiol. (London)* **268,** 757–773.
7. Kummer, T., Misgeld, T. & Sanes, J. R. (2006) *Curr. Opin. Neurobiol.* **16,** 74–82.
8. Gotti, C. & Clementi, F. (2004) *Prog. Neurobiol.* **74,** 363–396.
9. Colquhoun, L. M. & Patrick, J. W. (1997) *Adv. Pharmacol.* **39,** 191–220.
10. McCann, C. M., Bareyre, F. M., Lichtman, J. W. & Sanes, J. R. (2005) *BioTechniques* **38,** 945–952.
11. Miko, A., Werby, E., Sun, H., Healey, J. & Zhang, L. (2004) *J. Biol. Chem.* **279,** 22833–22840.
12. Wooltorton, J. R., Moss, S. J. & Smart, T. G. (1997) *Eur. J. Neurosci.* **9,** 2225–2235.
13. Sieghart, W. & Sperk, G. (2002) *Curr. Top. Med. Chem.* **2,** 795–816.
14. Connolly, C. N., Wooltorton, J. R., Smart, T. G. & Moss, S. J. (1996) *Proc. Natl. Acad. Sci. USA* **93,** 9899–9904.
15. Levandoski, M. M., Lin, Y., Moise, L., McLaughlin, J. T., Cooper, E. & Hawrot, E. (1999) *J. Biol. Chem.* **274,** 26113–26119.
16. Balass, M., Katchalski-Katzir, E. & Fuchs, S. (1997) *Proc. Natl. Acad. Sci. USA* **94,** 6054–6058.
17. Marinou, M. & Tzartos, S. J. (2003) *Biochem. J.* **372,** 543–554.
18. Biwersi, J. & Verkman, A. S. (1991) *Biochemistry* **30,** 7879–7883.
19. Baumann, S. W., Baur, R. & Sigel, E. (2001) *J. Biol. Chem.* **276,** 36275–36280.
20. Baumann, S. W., Baur, R. & Sigel, E. (2002) *J. Biol. Chem.* **277,** 46020–46025.
21. Chang, Y., Wang, R., Barot, S. & Weiss, D. S. (1996) *J. Neurosci.* **16,** 5415–5424.
22. Tretter, V., Ehya, N., Fuchs, K. & Sieghart, W. (1997) *J. Neurosci.* **17,** 2728–2737.
23. Orr-Urtreger, A., Goldner, F. M., Saeki, M., Lorenzo, I., Goldberg, L., De Biasi, M., Dani, J. A., Patrick, J. W. & Beaudet, A. L. (1997) *J. Neurosci.* **17,** 9165–9171.
24. Chen, D. & Patrick, J. W. (1997) *J. Biol. Chem.* **272,** 24024–24029.
25. Kawai, H., Zago, W. & Berg, D. K. (2002) *J. Neurosci.* **22,** 7903–7912.
26. Fabian-Fine, R., Skehel, P., Errington, M. L., Davies, H. A., Sher, E., Stewart, M. G. & Fine, A. (2001) *J. Neurosci.* **21,** 7993–8003.
27. Fuchs, S., Kasher, R., Balass, M., Scherf, T., Harel, M., Fridkin, M., Sussman, J. L. & Katchalski-Katzir, E. (2003) *Ann. N.Y. Acad. Sci.* **998,** 93–100.
28. Merlie, J. P. & Sebbanne, R. (1981) *J. Biol. Chem.* **256,** 3605–3608.